Inorganic Chemistry
Article

Inorg. Chem. **2011**, *50*, 1039–1046 **1039**
DOI: 10.1021/ic101779w

Chemical Bonding and Aromaticity in Trinuclear Transition-Metal Halide Clusters

Philippe F. Weck,*,† Alina P. Sergeeva,‡ Eunja Kim,§ Alexander I. Boldyrev,‡ and Kenneth R. Czerwinski†

†*Department of Chemistry and Harry Reid Center for Environmental Studies, University of Nevada—Las Vegas, 4505 Maryland Parkway, Las Vegas, Nevada 89154, United States,* ‡*Department of Chemistry and Biochemistry, Utah State University, Logan, Utah 84322-0300, United States, and* §*Department of Physics and Astronomy, University of Nevada—Las Vegas, 4505 Maryland Parkway, Las Vegas, Nevada 89154, United States*

Received September 1, 2010

Trinuclear transition-metal complexes such as Re_3X_9 (X = Cl, Br, I), with their uniquely featured structure among metal halides, have posed intriguing questions related to multicenter electron delocalization for several decades. Here we report a comprehensive study of the technetium halide clusters $[Tc_3(\mu\text{-}X)_3X_6]^{0/1-/2-}$ (X = F, Cl, Br, I), isomorphous with their rhenium congeners, predicted from density functional theory calculations. The chemical bonding and aromaticity in these clusters are analyzed using the recently developed adaptive natural density partitioning method, which indicates that only $[Tc_3X_9]^{2-}$ clusters exhibit aromatic character, stemming from a d-orbital-based π bond delocalized over the three metal centers. We also show that standard methods founded on the nucleus-independent chemical shift concept incorrectly predict the neutral Tc_3X_9 clusters to be aromatic.

Introduction

Elucidation of the crystal structure of anhydrous rhenium(III) chloride $ReCl_3$ by Cotton and Mague[1] marked a major milestone in the development of the field of metal−metal multiple bonds and transition-metal cluster chemistry.[2,3] The structure of ReX_3 (X = Cl, Br, I) compounds consists of $Re_3(\mu\text{-}X)_3X_6$ subunits with C_{3v} symmetry that exhibit a $[Re_3]^{9+}$ core.[1,4,5] The early proposal by Cotton and Haas[6] that Re═Re double bonds form the triangular diamagnetic $[Re_3]^{9+}$ core was largely substantiated by gas-phase photoelectron spectroscopy measurements and calculations of Re_3Cl_9 and Re_3Br_9 moieties.[7,8] Mass spectrometry experiments on ReX_3 (X = Cl, Br, I) also revealed that these compounds vaporize as Re_3X_9 clusters.[9−12] Upon vaporization of the compounds, the removal of up to three terminal halide ligands in the equatorial plane to yield Re_3X_9 species does not impact drastically the strength of the metal−metal bonds.

Although a wealth of information on the ground-state electronic structure of these clusters can be found in the literature, trinuclear metal cluster complexes such as Re_3X_9 also pose intriguing questions related to three-center electron delocalization. Correlating delocalized bonding properties of metal cluster complexes with their chemical reactivity is of paramount importance to understanding their catalytic activity. In an attempt to rationalize the remarkable stability of the $[Re_3]^{9+}$ core, Mealli and Proserpio proposed a double pattern of σ and π aromaticity in trinuclear rhenium clusters.[13] Recent theoretical studies have reinvestigated the aromaticity and chemical bonding of $[Re_3X_9]^{0/2-}$ (X = Cl, Br) clusters, resulting in contradictory conclusions regarding the aromaticity of the neutral complexes.[14−16]

While the structure of ReX_3 has been uniquely featured among metal halides for several decades, the recent discovery of $TcCl_3$,[17] isomorphous with $ReCl_3$, provides new opportunities

*To whom correspondence should be addressed. E-mail: weckp@unlv.nevada.edu.

(1) Cotton, F. A.; Mague, J. T. *Inorg. Chem.* **1964**, *3*, 1402.
(2) Cotton, F. A.; Walton, R. A. *Multiple Bonds Between Metal Atoms*, 2nd ed.; Oxford University Press: New York, 1993.
(3) Walton, R. A. *J. Cluster Sci.* **2004**, *15*, 559.
(4) Cotton, F. A.; Lippard, S. J. *Inorg. Chem.* **1965**, *4*, 59.
(5) Bennett, M. J.; Cotton, F. A.; Foxman, B. M. *Inorg. Chem.* **1968**, *7*, 1563.
(6) Cotton, F. A.; Haas, T. *Inorg. Chem.* **1964**, *3*, 10.
(7) Trogler, W. C.; Ellis, D. E.; Berkowitz, J. *J. Am. Chem. Soc.* **1979**, *101*, 5896.
(8) Bursten, B. E.; Cotton, F. A.; Green, J. C.; Seddon, E. A.; Stanley, G. G. *J. Am. Chem. Soc.* **1980**, *102*, 955.
(9) Rinke, K.; Schäfer, H. *Angew. Chem.* **1965**, *77*, 131.
(10) Büchler, A.; Blackburn, P. E.; Stauffer, J. L. *J. Phys. Chem.* **1966**, *70*, 685.
(11) Schäfer, H.; Rinke, K.; Rabeneck, H. *Z. Anorg. Allg. Chem.* **1974**, *403*, 23.
(12) Rinke, K.; Klein, M.; Schäfer, H. *J. Less-Common Met.* **1967**, *12*, 497.
(13) Mealli, C.; Proserpio, D. M. *Comm. Inorg. Chem.* **1989**, *9*, 37.
(14) Alvarado-Soto, L.; Ramírez-Tagle, R.; Arratia-Pérez, A. *Chem. Phys. Lett.* **2008**, *467*, 94.
(15) Alvarado-Soto, L.; Ramírez-Tagle, R.; Arratia-Pérez, A. *J. Phys. Chem. A* **2009**, *113*, 1671.
(16) Sergeeva, A. P.; Boldyrev, A. I. *Comments Inorg. Chem.* **2010**, *31*, 2.
(17) Poineau, F.; Johnstone, E. V.; Weck, P. F.; Kim, E.; Forster, P. M.; Scott, B. L.; Sattelberger, A. P.; Czerwinski, K. R. *J. Am. Chem. Soc.* **2010**, *132*, 15864.

Published on Web 12/29/2010

to critically analyze the interplay between structural properties, chemical bonding, and aromaticity in triangular M_3 metal atom clusters with another member of group VIIB elements. Similar to ReX_3 (X = Cl, Br, I), mass spectrometry experiments showed the presence of the $TcCl_3$ moiety in the gas phase from decomposition of the parent compound.[12] The scarcity of information available on technetium(III) halides compared to their rhenium congeners merely reflects the immaturity of technetium coordination chemistry, most of which is oriented toward the development of ^{99m}Tc-based agents for radiopharmaceutical imaging.[18,19]

In this paper, we report the comprehensive study of the structures of technetium halide clusters $[Tc_3(\mu\text{-}X)_3X_6]^{0/1-/2-}$ (X = F, Cl, Br, I) predicted from density functional theory (DFT) calculations. The chemical bonding and aromaticity in these clusters are analyzed using the recently developed adaptive natural density partitioning (AdNDP) method. For the sake of comparison with the present AdNDP analysis and with previous results for the $[Re_3Cl_9]^{0/2-}$ complexes,[14−16] we also utilize various methods based on the nucleus-independent chemical shift (NICS) concept to probe the aromaticity of representative $[Tc_3Cl_9]^{0/1-/2-}$ clusters.

Details of our computational approach are given in the next section, followed by a discussion and analysis of our results. A summary of our findings and conclusions is given in the last section.

Computational Methods

Structural Calculations. First-principles total-energy calculations were performed using the spin-polarized DFT, as implemented in the all-electron *DMol3* program[20] and the *Gaussian 09* software package.[21]

The exchange-correlation energy was calculated using the generalized gradient approximation[22] with the parametrization of Perdew and Wang[23] (PW91PW91). A combination of Becke's exchange functional[24] and the PW91 correlation functional (BPW91) was also used with *Gaussian 09* for the sake of comparison with recent calculations carried out at this level of theory on the $[Re_3Cl_9]^{0/2-}$ clusters.[16] For transition-metal cluster computations, pure functionals such as the PW91 and Becke's are generally preferred over hybrid functionals that appear to describe metal−metal bonds less accurately.[25,26] In particular, the PW91 functional was found to accurately reproduce structural parameters of various technetium-containing structures characterized experimentally.[17,27−29] Double numerical basis sets including polarization functions on all atoms (DNP) with scalar relativistic corrections applied were used in all of the *DMol3* calculations. The SDD and LANL2DZ basis sets were used in the *Gaussian 09* calculations (see the Supporting Information for details). Optimized geometries were obtained using direct inversion in a subspace method (DIIS) without symmetry constraints with an energy convergence tolerance of 10^{-5} hartree and a gradient convergence of 10^{-3} hartree/bohr. The energy tolerance in the self-consistent-field calculations was set to 10^{-6} hartree.

AdNDP Method. We performed the chemical-bonding analyses of all of the $[Tc_3X_9]^{0/2-}$ (X = F, Cl, Br, I) complexes using the AdNDP method, which has been recently developed by Zubarev and Boldyrev.[30] This method has been successfully applied to a series of all-boron clusters,[30] aromatic organic molecules,[31] gold clusters,[32] and transition-metal clusters and condensed-phase materials.[16,33,34] The AdNDP method is based on the concept of an electron pair being the main element of the chemical-bonding model. The AdNDP method represents the electronic structure in terms of *n*-center two-electron (*n*c-2e) bonds, with *n* spanning from one to the total number of atoms in the system of interest. The AdNDP program reveals both localized Lewis bonding elements (1c-2e objects, corresponding to core electrons and lone pairs, and 2c-2e objects, corresponding to two-center two-electron bonds) and delocalized bonding elements (*n*c-2e objects, $n \geq 3$), which are associated with the concepts of aromaticity and antiaromaticity. The reader can find a detailed description of the method elsewhere.[30] Details of the calculations associated with the AdNDP analysis are given in the Supporting Information.

NICS Methods. Several methods based on the NICS concept were also utilized to investigate the aromaticity of the clusters.

Specifically, we employed the widely used NICS approach proposed by Elser and Haddon[35] and developed by Schleyer et al.[36] In its original formulation, NICS is defined as the absolute magnetic shielding calculated at the ring center, NICS(0), with the sign of the computed value reversed to correspond to the usual NMR chemical shift convention.[36] Negative NICS values indicate the presence of diatropic ring currents, interpreted as aromaticity, whereas positive NICS values denote paratropic ring currents, associated with antiaromaticity. The NICS(1) index, which is calculated for a ghost atom located 1 Å above the ring center, is also routinely used as a probe of π aromaticity. This index was introduced in order to limit the effect of the local σ-bonding contributions typically contained within the NICS(0) index.[38,39]

The NICS rate variant recently introduced by Noorizadeh and Dardab[37] to correlate the aromaticity of cyclic complexes with variation of the NICS index at different distances from the ring center was also used in this study. The presence of a maximum (minimum) in the NICS-rate curve is interpreted as an aromatic (antiaromatic) character of the cyclic complex. If the NICS-rate curve features both a maximum and a minimum, the NICS-rate ratio NRR = |max(NICS rate)|/|min(NICS rate)| can be considered as a measure of the aromaticity.[37] Details of the NICS calculations are given in the Supporting Information.

Results and Discussion

Structural Results. All structures optimized for the neutral and singly and doubly charged $[Tc_3(\mu\text{-}X)_3X_6]^{0/1-/2-}$

(18) Storr, T.; Thompson, K. H.; Orvig, C. *Chem. Soc. Rev*. **2006**, *35*, 534.
(19) Tisato, F.; Porchia, M.; Bolzati, C.; Refosco, F.; Vittadini, A. *Coord. Chem. Rev*. **2006**, *250*, 2034.
(20) Delley, B. *J. Chem. Phys*. **2000**, *113*, 7756.
(21) Frisch, M. J. et al. . *Gaussian 09*, revision A.02; Gaussian, Inc.: Wallingford, CT, 2009.
(22) Perdew, J. P.; Chevary, J. A.; Vosko, S. H.; Jackson, K. A.; Pederson, M. R.; Singh, D. J.; Fiolhais, C. *Phys. Rev. B* **1992**, *46*, 6671.
(23) Perdew, J. P.; Wang, Y. *Phys. Rev. B* **1992**, *45*, 13244.
(24) Becke, A. D. *Phys. Rev. A* **1988**, *38*, 3098.
(25) Gutsev, G. L.; Bauschlicher, C. W., Jr. *J. Phys. Chem. A* **2003**, *107*, 7013.
(26) Furche, F.; Perdew, J. P. *J. Chem. Phys*. **2006**, *124*, 044103.
(27) Weck, P. F.; Kim, E.; Poineau, F.; Rodriguez, E.; Sattelberger, A. P.; Czerwinski, K. R. *Inorg. Chem*. **2009**, *48*, 6555.
(28) Poineau, F.; Weck, P. F.; Forster, P.; Sattelberger, A. P.; Czerwinski, K. R. *Dalton Trans*. **2009**, 10338.
(29) Weck, P. F.; Kim, E.; Poineau, F.; Rodriguez, E. E.; Sattelberger, A. P.; Czerwinski, K. R. *Dalton Trans*. **2010**, *39*, 7207.
(30) Zubarev, D. Yu.; Boldyrev, A. I. *Phys. Chem. Chem. Phys*. **2008**, *10*, 5207–5217.
(31) Zubarev, D. Yu.; Boldyrev, A. I. *J. Org. Chem*. **2008**, *73*, 9251–9258.
(32) Zubarev, D. Yu.; Boldyrev, A. I. *J. Phys. Chem. A* **2009**, *113*, 866–868.
(33) Sergeeva, A. P.; Averkiev, B. B.; Boldyrev, A. I. In *Metal−Metal Bonding*; Structure and Bonding Book Series; Parkin, G., Ed.; Springer: Berlin/Heidelberg, 2010; Vol. *136*, pp 275−306.
(34) Sergeeva, A. P.; Boldyrev, A. I. *Phys. Chem. Chem. Phys*. **2010**, *12*, 12050–12054.
(35) Elser, V.; Haddon, R. C. *Nature* (*London*) **1987**, *325*, 792.
(36) Schleyer, P. v. R.; Maerker, C.; Dransfeld, A.; Jiao, H.; van Eikema Hommes, N. J. R. *J. Am. Chem. Soc*. **1996**, *118*, 6317.
(37) Noorizadeh, S.; Dardab, M. *Chem. Phys. Lett*. **2010**, *493*, 376.
(38) Aihara, J. *Chem. Phys. Lett*. **2002**, *365*, 34.
(39) Lazzeretti, P. *Phys. Chem. Chem. Phys*. **2004**, *6*, 217.

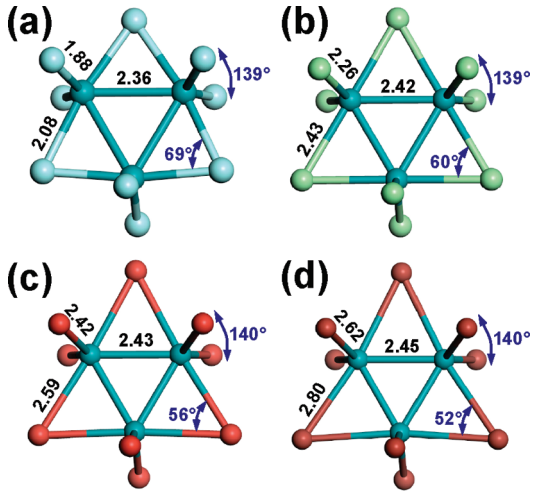

Figure 1. Ball-and-stick models of the D_{3h}-symmetry equilibrium conformers of the neutral clusters $Tc_3(\mu\text{-}X)_3X_6$ (X = F, Cl, Br, I) computed at the PW91PW91/DNP level of theory: (a) Tc_3F_9; (b) Tc_3Cl_9; (c) Tc_3Br_9; (d) Tc_3I_9.

(X = F, Cl, Br, I) clusters possess D_{3h} symmetry and correspond to low-spin configurations, i.e., singlet ground states for $[Tc_3X_9]^{0/2-}$ and doublet ground states for $[Tc_3X_9]^{-}$, consistent with the marked propensity of technetium to form low-spin complexes.[40] Previous studies of $[Re_3X_9]^{0/2-}$ (X = Cl, Br) clusters in the gas phase showed similar symmetry and electronic characteristics.[8,15] Equilibrium conformers of the neutral Tc_3X_9 clusters computed at the PW91PW91/DNP level of theory are displayed in Figure 1. Isomorphous with their rhenium congeners, all tritechnetium nonahalide clusters feature a planar arrangement of the triangular Tc_3 core with three equatorial bridging halide ligands (μ^2-X) and six apical halide atoms (out-of-plane). Structural parameters for the equilibrium geometries of the $[Tc_3X_9]^{0/1-/2-}$ (X = F, Cl, Br, I) clusters computed at different levels of theory using the *DMol3* and *Gaussian 09* software packages are given in Table 1. Excellent overall agreement between the different theoretical treatments is obtained, with differences in the calculated bond distances and angles typically less than 0.03 Å and 4°, respectively. Therefore, in the discussion of the structural results below, similar trends appear at different levels of theory.

In all of the clusters, the Tc−X bond distances tend to increase linearly with the effective ionic radius of the halogen ion with formal charge 1−, i.e., $r_F = 1.33$ Å, $r_{Cl} = 1.81$ Å, $r_{Br} = 1.96$ Å, and $r_I = 2.20$ Å.[41] The shortest Tc−X bond length corresponds to the bonds between Tc and the apical X ligands. The Tc−Tc bond distances also increases linearly, with a gentler variation, as the electronegativity of the surrounding halogen atoms decreases and the atomic radius increases down the halogen series. The coordination of the Tc_3 core by chelating halide ligands tends to symmetrize the triangular core (D_{3h} conformation) and elongate the Tc−Tc bonds compared to the naked Tc_3 cluster with C_s symmetry and an average side length of 2.24 Å corresponding to a sextet ground state.[42] The higher symmetry of the Tc_3 core upon chelation can essentially be viewed as an antagonistic effect of the lowering of its spin configuration from a sextet to a singlet/doublet ground state.[43] All bond lengths show a tendency to slightly increase by less than 0.1 Å as the charge of the clusters varies from neutral to doubly charged. This charge variation is also accompanied by a significant decrease of the X−Tc−X angles between metal atoms and apical halides, while the Tc−μ-X−Tc bridging angles remain nearly unchanged. However, the bridging angles decrease gradually from ≈69° to ≈52° as the effective ionic radius of the halogen ligands increases from fluorine to iodine.

Although the $TcCl_3$ compound (space group $R\bar{3}m$; $Z = 18$) recently characterized by X-ray diffraction (XRD) is built up on Tc_3Cl_9 units with C_{3v} symmetry,[17] a close structural relationship exists between these units and the gas-phase D_{3h}-symmetry Tc_3Cl_9 cluster with coordinately unsaturated technetium atoms. The Tc−Tc, Tc−μ-Cl, and Tc−Cl bond distances in the Tc_3Cl_9 cluster calculated to be 2.413, 2.504, and 2.313 Å at the BPW91/LANL2DZ level are in fair agreement with their counterparts in the crystal, i.e., 2.4445, 2.3731, and 2.2375 Å, respectively. Residual discrepancies can be ascribed to the presence of chemically distinct intercluster Tc−X bonds forming bridge rhomboids in the crystal with bond lengths of 2.3733 and 2.5852 Å for the Tc−Cl(apical) and Tc−Cl-(equatorial) bonds.

AdNDP Analysis. The AdNDP program has revealed the same chemical-bonding elements for all of the $[Tc_3X_9]^{0/2-}$ (X = F, Cl, Br, I) complexes as those in the chemical-bonding analysis performed for Re_3Cl_9 and $[Re_3Cl_9]^{2-}$,[16] with the only difference being in the occupation numbers (ONs) of the revealed *n*c-2e objects. The ONs indicate how many electrons there are per bond. The ONs of all of the recovered chemical-bonding elements are close to the ideal limit of 2.00 |e|. We present a visualization of the results of the AdNDP analysis for $[Tc_3Cl_9]^{0/2-}$ only; see Figure 2 for the AdNDP analysis of Tc_3Cl_9 and Figure 3 for the AdNDP analysis of $[Tc_3Cl_9]^{2-}$. The ONs for all of the revealed *n*c-2e objects on the $[Tc_3X_9]^{0/2-}$ (X = F, Cl, Br, I) complexes are listed in Table 2.

According to the AdNDP analysis, there are 42 valence two-electron objects in Tc_3Cl_9 (see Figure 2). These objects are as follows: 27 lone pairs of ON = 1.68−1.99 |e| (three on each of the chlorine atoms), 6 2c-2e p−d-hybridized σ bonds between each apical chlorine atom and the neighboring technetium atom of ON = 1.94 |e|, 3 3c-2e σ bonds holding together bridging chlorine atoms with two neighboring technetium atoms of ON = 1.94 |e| (the major electron density contribution of 75% to these 3c-2e Tc−Cl−Tc σ bonds comes from lone pairs on bridging μ-chlorine atoms; in other words, if these three 3c-2e Tc−Cl−Tc σ bonds are reduced to just lone pairs on the three bridging μ-chlorine atoms, their ONs drop to 1.46 |e|), 3 2c-2e d-atomic-orbital (d-AO)-based Tc−Tc σ bonds of ON = 1.99 |e|, and 3 2c-2e d-AO-based Tc−Tc π bonds of ON = 1.99 |e|. The low ON values of the lone

(40) Schwochau, K. *Technetium: Chemistry and Radiopharmaceutical Applications*; Wiley-VCH: New York, 2000.
(41) Shannon, R. D. *Acta Crystallogr.* **1976**, *A32*, 751.
(42) Weck, P. F.; Kim, E.; Czerwinski, K. R.; Tománek, D. *Phys. Rev. B* **2010**, *81*, 125448.
(43) Weck, P. F.; Kim, E.; Poineau, F.; Czerwinski, K. R. *Phys. Chem. Chem. Phys.* **2009**, *11*, 10003.

Table 1. Structural Parameters of $[Tc_3(\mu\text{-}X)_3X_6]^{0/1-/2-}$ (X = F, Cl, Br, I) Clusters with D_{3h} Symmetry Calculated Using DFT

		distances (Å)			angles (deg)	
cluster	method	Tc−Tc	Tc−μ-X	Tc−X	Tc−μ-X−Tc	X−Tc−X
Tc_3F_9	DMol/PW91PW91/DNP	2.363	2.079	1.879	69.2	138.9
	G09/PW91PW91/SDD	2.349	2.089	1.895	68.4	139.4
	G09/BPW91/LANL2DZ	2.366	2.103	1.897	68.6	141.1
$[Tc_3F_9]^-$	DMol/PW91PW91/DNP	2.385	2.099	1.917	69.2	131.6
	G09/PW91PW91/SDD	2.368	2.105	1.934	68.5	133.4
	G09/BPW91/LANL2DZ	2.388	2.115	1.934	68.6	132.6
$[Tc_3F_9]^{2-}$	DMol/PW91PW91/DNP	2.424	2.125	1.968	69.5	122.6
	G09/PW91PW91/SDD	2.402	2.126	1.982	68.8	126.4
	G09/BPW91/LANL2DZ	2.423	2.138	1.982	69.0	126.5
Tc_3Cl_9	DMol/PW91PW91/DNP	2.419	2.433	2.259	59.6	138.8
	G09/PW91PW91/SDD	2.397	2.478	2.293	57.8	141.5
	G09/BPW91/LANL2DZ	2.413	2.504	2.313	57.6	143.0
$[Tc_3Cl_9]^-$	DMol/PW91PW91/DNP	2.441	2.440	2.295	60.0	133.6
	G09/PW91PW91/SDD	2.416	2.483	2.329	58.2	136.1
	G09/BPW91/LANL2DZ	2.433	2.506	2.349	58.1	135.8
$[Tc_3Cl_9]^{2-}$	DMol/PW91PW91/DNP	2.477	2.447	2.343	60.8	127.8
	G09/PW91PW91/SDD	2.449	2.488	2.377	59.0	130.3
	G09/BPW91/LANL2DZ	2.468	2.512	2.396	58.8	128.8
Tc_3Br_9	DMol/PW91PW91/DNP	2.435	2.591	2.417	56.1	139.9
	G09/PW91PW91/SDD	2.415	2.609	2.425	55.1	139.2
	G09/BPW91/LANL2DZ	2.430	2.642	2.456	54.8	141.3
$[Tc_3Br_9]^-$	DMol/PW91PW91/DNP	2.456	2.595	2.451	56.5	134.6
	G09/PW91PW91/SDD	2.433	2.609	2.461	55.6	135.4
	G09/BPW91/LANL2DZ	2.448	2.642	2.492	55.2	136.2
$[Tc_3Br_9]^{2-}$	DMol/PW91PW91/DNP	2.491	2.602	2.497	57.2	129.0
	G09/PW91PW91/SDD	2.466	2.608	2.507	56.4	131.0
	G09/BPW91/LANL2DZ	2.480	2.642	2.541	56.0	130.4
Tc_3I_9	DMol/PW91PW91/DNP	2.454	2.801	2.624	51.9	139.7
	G09/PW91PW91/SDD	2.433	2.808	2.622	51.3	138.8
	G09/BPW91/LANL2DZ	2.450	2.820	2.635	51.5	139.2
$[Tc_3I_9]^-$	DMol/PW91PW91/DNP	2.472	2.803	2.656	52.3	135.7
	G09/PW91PW91/SDD	2.449	2.805	2.656	51.8	135.8
	G09/BPW91/LANL2DZ	2.464	2.817	2.670	51.8	136.3
$[Tc_3I_9]^{2-}$	DMol/PW91PW91/DNP	2.503	2.808	2.698	52.9	131.6
	G09/PW91PW91/SDD	2.480	2.799	2.698	52.6	132.7
	G09/BPW91/LANL2DZ	2.493	2.811	2.713	52.6	132.7

pairs on some of the chlorine atoms ($p_{tangential}$ bridging and p_{radial} apical) are signs that those electron pairs tend to be more delocalized. Nevertheless, we include them in our chemical-bonding picture as lone pairs because more than 80% of the electron density is contributed by the chlorine atoms.

In the case of doubly charged $[Tc_3Cl_9]^{2-}$, 86 valence electrons form 43 two-electron objects (see Figure 3): 27 lone pairs of ON = 1.73−1.99 |e| (three on each of the chlorine atoms), 6 2c-2e p−d-hybridized Tc−Cl σ bonds of ON = 1.99 |e|, 3 3c-2e Tc−Cl−Tc σ bonds of ON = 1.97 |e|, 3 2c-2e d-AO-based Tc−Tc σ bonds of ON = 1.97 |e|, 3 lone pairs of "$d_{tangential}$"-type on technetium atoms of ON = 1.86 |e|, and 1 delocalized d_{radial}-AO-based π bond, which can be viewed as being delocalized over three technetium atoms (3c-2e π bond of ON = 1.60 |e|) or more precisely as delocalized over technetium and apical chlorine atoms (9c-2e π bond of ON = 2.00 |e|). The AdNDP analysis is performed in a way that for a given molecule bonds are picked out whose ONs exceed the established threshold value, usually close to 2.00 |e|, with the bonds of lower ONs being discarded. Nevertheless, the threshold values can be set individually for each nc-2e bond (n = 1, 2, ... number of atoms in a molecule) to ensure flexibility of the algorithm. In the case of the AdNDP analysis of the $[Tc_3Cl_9]^{2-}$ dianion, the 3c-2e π bond can be recovered with ON=1.60 |e| by varying the threshold for 3c-2e bonds to allow acceptance of the bonds with low ONs. We view the 3c-2e π bond as the zeroth-order description of delocalized π bonding because the ON value of this bond is low compared to the ideal value of 2.00 |e|. The more accurate description of the delocalized π bonding can be obtained if the threshold on the 3c-2e bonds is set so that only bonds with high ONs are accepted (3 × 3c-2e Tc−Cl−Tc σ bonds of ON = 1.97 |e|), while the 3c-2e π bond of ON = 1.60 |e| is discarded and found to be delocalized over nine centers with ON = 2.00 |e| instead (see the 9c-2e π bond; Figure 3). Similar to the case of the chemical-bonding picture of neutral Tc_3X_9 complexes, the $p_{tangential}$-bridging lone pairs on chlorine atoms have low ON values. However, we include these electron pairs in the chemical-bonding picture because the main contribution (more than 80%) to the electron density comes from the chlorine atoms.

As the reader may notice, the difference in the chemical-bonding picture of neutral and doubly charged Tc_3Cl_9 and $[Tc_3Cl_9]^{2-}$ is rooted in the AdNDP bonds formed out of d-AO-based canonical π molecular orbitals (π-MOs). There are three occupied d-AO-based π-MOs in neutral Tc_3Cl_9, with the main electron density contribution coming from the d-AOs of technetium atoms: totally bonding radial π-MO of a_2'' symmetry and a pair of degenerate π-MOs of e″ symmetry. According to the AdNDP analysis, these three π-MOs are responsible for the formation of three consecutive 2c-2e Tc−Tc π bonds of ON = 1.86 |e|. We believe that a molecule should be considered as being

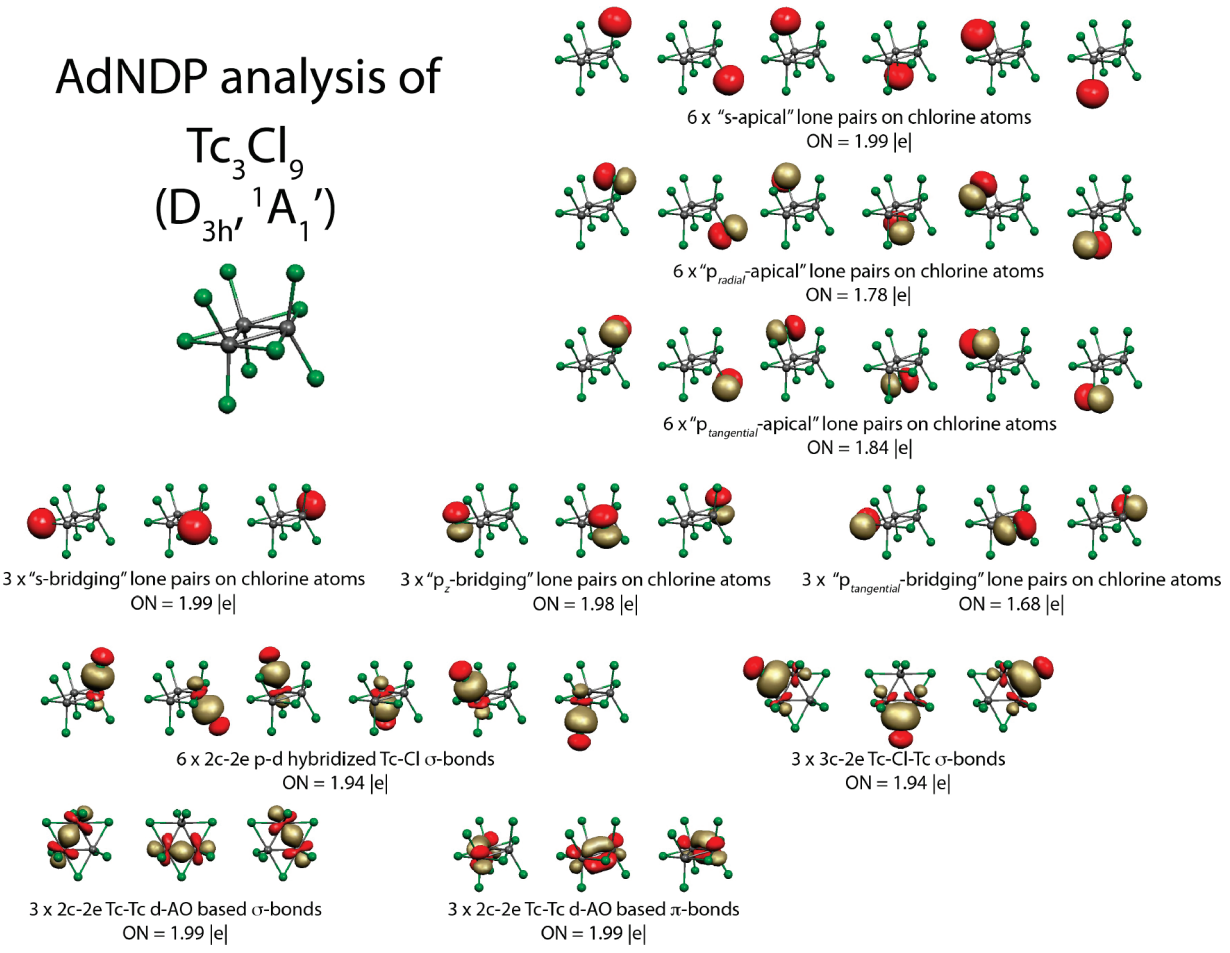

Figure 2. Chemical-bonding elements revealed by the AdNDP analysis of the neutral Tc_3Cl_9. The ONs are reported at the BPW91/LANL2DZ level of theory.

aromatic only if there is a delocalized bonding encountered in a cyclic system by means of the AdNDP analysis. Because the completely delocalized three canonical π-MOs are localized into 2c-2e Tc−Tc π bonds by means of the AdNDP analysis, the neutral Tc_3Cl_9 species is not π aromatic. In the case of doubly charged $[Tc_3Cl_9]^{2-}$, there are four occupied d-AO-based π-MOs, with the main electron density contribution coming from the d-AOs of technetium atoms: totally bonding radial π-MO of a_2'' symmetry, a pair of degenerate π-MOs of e'' symmetry, and totally antibonding tangential π-MO of a_1'' symmetry. The addition of two excess electrons to the totally antibonding π-tangential $2a_1''$ lowest unoccupied molecular orbital of Tc_3Cl_9 to produce doubly charged $[Tc_3Cl_9]^{2-}$ changes the chemical-bonding picture distinctly (Figure 3 compared to Figure 2). A detailed discussion of the canonical molecular orbital (CMO) analysis elucidating the order of CMO occupation, particularly why a completely antibonding tangential a_1'' CMO is occupied before the other set of doubly degenerate e'' CMOs, can be found elsewhere on an example of isoelectronic $[Re_3Cl_9]^{0/2-}$ species.[16] The AdNDP method revealed that the density associated with these four d-AO-based π-MOs in the case of the $[Tc_3Cl_9]^{2-}$ cluster can be considered as three lone pairs (ON = 1.86 |e|) on technetium atoms and a totally bonding 3c-2e π bond of ON = 1.60 |e|. Even though there are 8 electrons comprising π-CMOs, we apply the $4n + 2$ Hückel's rule only to those π electrons, which are involved in delocalized π bonding, and disregard those of the localized objects (three lone pairs in the case of $[Tc_3Cl_9]^{2-}$). The $[Tc_3Cl_9]^{2-}$ cluster is, thus, π aromatic, with the two electrons of the 3c-2e π bond satisfying the $4n + 2$ Hückel's rule for aromaticity ($n = 0$). The low value of the ON for the d-AO-based π bond means that this bond is delocalized over more than just three technetium atoms. If we allow the AdNDP method to increase the number of atoms on which the π bond can be delocalized, this bond can be found as a 9c-2e π bond with ON = 2.00 |e|, now also involving the electron density coming from apical chlorine atoms (Figure 3).

Strictly speaking, the 9c-2e description of the delocalized π bonding in $[Tc_3Cl_9]^{2-}$ is more accurate for the ON if the 9c-2e π bond is higher than that of the 3c-2e π bond, but one needs to keep in mind that the major contribution of the electron density to the delocalized π bonding is coming from technetium atoms (80%). In other words, the delocalized π bonding responsible for π aromaticity in the $[Tc_3Cl_9]^{2-}$ dianion as the d_{radial}-AO-based 3c-2e π bond delocalized over three technetium atoms can be viewed as the zeroth-order approximation.

We stress once again that a molecule should be considered as being aromatic/antiaromatic only if delocalized bonding is encountered in a cyclic system by means of the AdNDP analysis. If there are $4n + 2/4n$ σ, π, δ, or φ

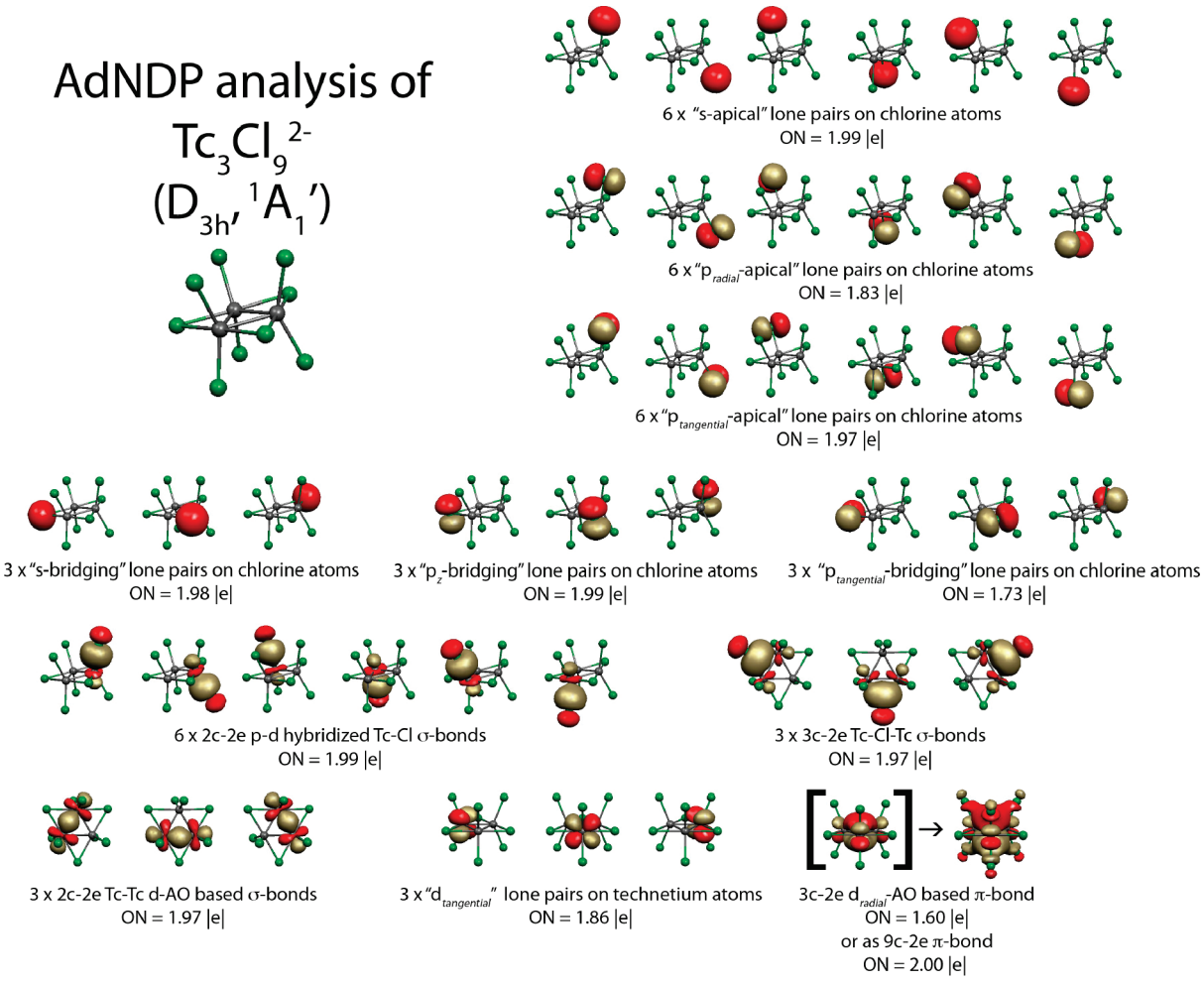

Figure 3. Chemical-bonding elements revealed by the AdNDP analysis of the $[Tc_3Cl_9]^{2-}$ dianion. The ONs are reported at the BPW91/LANL2DZ level of theory.

Table 2. ONs of the Revealed *nc*-2e Objects on All of the $[Tc_3X_9]^{0/2-}$ (X = F, Cl, Br, I) Complexes Obtained Using the AdNDP program[a]

	neutral Tc_3X_9 complexes				doubly charged $[Tc_3X_9]^{2-}$ complexes			
nc-2e object	Tc_3F_9	Tc_3Cl_9	Tc_3Br_9	Tc_3I_9	$[Tc_3F_9]^{2-}$	$[Tc_3Cl_9]^{2-}$	$[Tc_3Br_9]^{2-}$	$[Tc_3I_9]^{2-}$
				Lone Pairs on Halogen Atoms				
"s apical"	1.99	1.99	1.99	1.98	1.99	1.99	1.99	1.98
"p_{radial} apical"	1.85	1.78	1.76	1.77	1.88	1.83	1.83	1.88
"$p_{tangential}$ apical"	1.88	1.84	1.83	1.89	1.97	1.97	1.97	1.97
"s bridging"	1.99	1.99	1.98	1.98	1.99	1.98	1.98	1.98
"p_z bridging"	1.99	1.98	1.99	1.99	1.98	1.99	1.98	1.99
"$p_{tangential}$ bridging"	1.77	1.68	1.65	1.61	1.82	1.73	1.71	1.69
				Lone Pairs on Technetium Atoms				
"$d_{tangential}$"					1.82	1.86	1.86	1.88
				Bonding Elements				
2c-2e Tc−X σ bonds	2.00	1.94	1.93	1.93	2.00	1.99	1.93	1.99
3c-2e Tc−X−Tc σ bonds	1.97	1.94	1.93	1.91	1.98	1.97	1.96	1.95
2c-2e Tc−Tc σ bonds	1.98	1.99	1.99	1.99	1.98	1.97	1.97	1.97
2c-2e Tc−Tc π bonds	1.93	1.99	1.99	1.99				
[3c-2e] → 9c-2e π bonds					[1.77] → 2.00	[1.60] → 2.00	[1.57] → 2.00	[1.52] → 2.00

[a] ONs are given in |e| units.

electrons involved in delocalized bonding in a cyclic system, the molecule should be considered as σ, π, δ, or φ aromatic/antiaromatic regardless of whether s-, p-, d-, or f-AO-based σ, π, δ, or φ electron density is discussed (assuming that no mixing of the tangential and radial orbitals occurs). The rigorous reader may want to consult reference 33 for the counting rules of s-, p-, d-, and f-AO-based σ, π, δ, or φ aromaticity/antiaromaticity in model

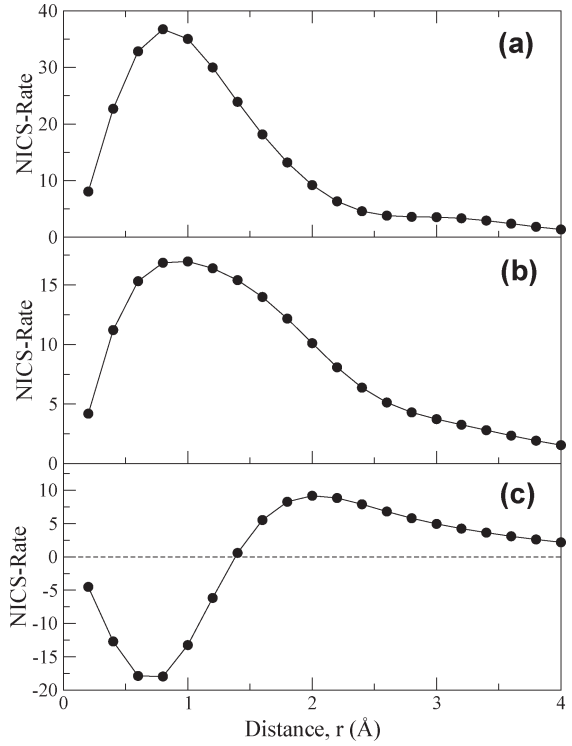

Figure 4. Evolution of the NICS rate as a function of the normal distance r from the ring center for (a) Tc_3Cl_9, (b) $[Tc_3Cl_9]^-$, and (c) $[Tc_3Cl_9]^{2-}$. NICS values were computed using the GIAO method at the BPW91/LANL2DZ level of theory.

triatomic and tetraatomic cyclic systems with a mixing of the tangential and radial orbitals taken into account.

NICS Analysis. Similar to the case of the 5d transition-metal clusters $[Re_3X_9]^{0/2-}$ (X = Cl, Br) studied recently,[15] the negative NICS(0) and NICS(1) values calculated for $[Tc_3X_9]^{0/2-}$ (X = Cl, Br) are indicative of d-orbital aromaticity. The values computed with the GIAO method at the BPW91/LANL2DZ level of theory are as follows (in ppm): NICS(0) = −53.34 and NICS(1) = −26.26 for Tc_3Cl_9; NICS(0) = −2.83 and NICS(1) = −16.08 for $[Tc_3Cl_9]^{2-}$; NICS(0) = −60.41 and NICS(1) = −30.45 for Tc_3Br_9; NICS(0) = −19.50 and NICS(1) = −30.33 for $[Tc_3Br_9]^{2-}$. While the aromaticity predicted for $[Tc_3X_9]^{2-}$ (X = Cl, Br) appears to agree with the results of the AdNDP chemical-bonding analysis reported above, the NICS(0) and NICS(1) indices erroneously suggest an aromatic character of the Tc_3X_9 neutral clusters, not observed in the AdNDP analysis. Similar discrepancies between results derived from standard NICS approaches and the AdNDP analysis were also reported for Re_3Cl_9.[16]

The alternative NICS-rate method proposed by Noorizadeh and Dardab[37] to probe the aromaticity of cyclic complexes was also utilized. Figure 4 displays the evolution of the computed NICS rate as a function of the normal distance r from the ring center for the $[Tc_3Cl_9]^{0/1-/2-}$ clusters. As shown in parts a and b of Figure 4, both Tc_3Cl_9 and $[Tc_3Cl_9]^-$ clusters are predicted to be highly aromatic and exhibit NICS-rate maxima of +36.74 (r = 0.8 Å) and +16.97 (r = 1.0 Å), respectively. Like the standard NICS indices, the NICS-rate index fails to predict the nonaromatic character of the Tc_3Cl_9 neutral cluster. Variation of the NICS rate for the $[Tc_3Cl_9]^{2-}$ cluster features a minimum of −17.97 at r = 0.8 Å and a maximum of +9.18 at r = 2.0 Å (cf. Figure 4c). The presence of a minimum and a maximum in the NICS-rate curve implies that some degree of competition between σ and π electrons takes place in the system. The effect of σ electrons steadily diminishes as the normal distance r from the ring center increases, while the effect of π electrons increases quickly to reach its maximum at r = 2.0 Å and slowly vanishes asymptotically. The value of the resulting NICS-rate ratio, NRR = 0.51, suggests that $[Tc_3Cl_9]^{2-}$ is at the boundary between nonaromatic and weakly aromatic character.[37] Thus, no decisive conclusion can be reached regarding the aromaticity of this complex, unlike with the AdNDP chemical-bonding analysis and the NICS(0) and NICS(1) indices, which unambiguously predict an aromatic character. Therefore, the recently proposed NICS-rate approach might not be valid to assess the aromatic nature of transition-metal-bearing clusters, although this method showed some success for cyclic organic complexes.

A growing number of studies have shown that no single indicator of aromaticity works properly for all cyclic complexes and emphasized the need for using systematically more than a single index to analyze the aromaticity.[39,44−50] Even if several indicators are used, a definite conclusion of the local ring aromaticity might not always be reached if different indicators yield different results. These observations further demonstrate the importance of the development of new comprehensive methods such as the AdNDP approach to correctly assess the bonding and aromaticity of nonclassical molecular systems with delocalized bonding.

Conclusion

Using DFT, we have carried out a comprehensive study of the technetium halide clusters $[Tc_3(\mu\text{-}X)_3X_6]^{0/1-/2-}$ (X = F, Cl, Br, I) with D_{3h} symmetry. Structural data for the Tc_3Cl_9 neutral clusters calculated at several levels of theory are in close agreement with XRD data available for the $Tc_3(\mu\text{-}Cl)_3Cl_6$ compound crystallizing in the space group $R\bar{3}m$. We hope that the predicted neutral technetium halide species (Tc_3X_9, X = F, Br, and I) will soon be synthesized.

The chemical bonding and aromaticity in these clusters are analyzed using the recently developed AdNDP method, which indicates that only $[Tc_3X_9]^{2-}$ clusters exhibit aromatic character, stemming from a d-orbital-based π bond delocalized over the three metal centers. Specifically, the AdNDP chemical-bonding analysis revealed 42 valence two-electron objects in all of the neutral Tc_3X_9 (X = F, Cl, Br, I) complexes, among which 27 are nonbonding elements, i.e., three lone pairs on each of the 12 halogen atoms, and 15 are bonding elements, i.e., 6 2c-2e Tc−X σ bonds, 3 3c-2e Tc−X−Tc σ bonds, 3 2c-2e d-AO-based Tc−Tc σ bonds, and 3 2c-2e

(44) Viglione, R. G.; Zanasi, R. *Org. Lett*. **2004**, *6*, 2265–2267.
(45) Faglioni, F.; Ligabue, A.; Pelloni, S.; Soncini, A.; Viglione, R. G.; Ferraro, M. B.; Zanasi, R.; Lazzeretti, P. *Org. Lett*. **2005**, *7*, 3457–3460.
(46) Osuna, S.; Poater, J.; Bofill, J. M.; Alemany, P.; Solà, M. *Chem. Phys. Lett*. **2006**, *428*, 191–195.
(47) Feixas, F.; Jiménez-Halla, J. O. C.; Matito, E.; Poater, J.; Solà, M. *Pol. J. Chem*. **2007**, *81*, 783–797.
(48) Feixas, F.; Matito, E.; Poater, J.; Solà, M. *J. Phys. Chem. A* **2007**, *111*, 4513–4521.
(49) Islas, R.; Martínez-Guajardo, G.; Jiménez-Halla, J. O. C.; Solà, M.; Merino, G. *J. Chem. Theory Comput*. **2010**, *6*, 1131–1135.
(50) Castro, A. C.; Osorio, E.; Jiménez-Halla, J. O. C.; Matito, E.; Tiznado, W.; Merino, G. *J. Chem. Theory Comput*. **2010**, *6*, 2701–2705.

d-AO-based Tc−Tc π bonds. In the case of doubly charged $[Tc_3X_9]^{2-}$ anions, 43 two-electron objects were found, among which 30 are nonbonding elements, i.e., 27 lone pairs on the halogen atoms and 3 lone pairs on technetium atoms, and 13 are bonding elements, i.e., 6 2c-2e Tc−X σ bonds, 3 3c-2e Tc−X−Tc σ bonds, 3 2c-2e d-AO-based Tc−Tc σ bonds, and a 3c-2e d-AO-based π bond delocalized over three technetium atoms responsible for aromaticity in these dianionic complexes.

We also show that methods based on the NICS concept, such as the NICS(0)-, NICS(1)-, and NICS-rate approaches, incorrectly predict the neutral Tc_3X_9 clusters to be aromatic. These results further demonstrate the importance of the development of new methods such as the AdNDP approach to correctly assess the bonding and aromaticity of nonclassical molecular systems with delocalized bonding.

Acknowledgment. Funding for the research performed at UNLV was provided by the U.S. Department of Energy, Basic Energy Sciences SISGR, Contract 47824B and Agreement DE-FG52-06NA26399. The work done at USU was supported by the National Science Foundation (Grant CHE-0714851).

Supporting Information Available: Details of the computational methods and complete reference for ref 21. This material is available free of charge via the Internet at http://pubs.acs.org.